

Article

Orbital Regularity of Exoplanets and the Symmetries of the Kepler Problem

József Cseh ^{1,*}, Phong Dang ^{1,2,†}, Sándor Szilágyi ¹ and Géza Lévai ¹

¹ Institute for Nuclear Research, P.O. Box 51, 4001 Debrecen, Hungary; pdang5@lsu.edu (P.D.); sandor.szilagyi@altmail.se (S.S.); levai@atomki.hu (G.L.)

² Faculty of Science and Technology, University of Debrecen, 4032 Debrecen, Hungary

* Correspondence: cseh@atomki.hu

† Current address: Department of Physics and Astronomy, Louisiana State University, Baton Rouge, LA 70802, USA.

Abstract: We investigate the question whether or not the orbitals of exoplanets follow the symmetry-governed sequence found by Barut from the dynamical group of the Kepler problem. In particular, we consider their star distances, periods, and velocities. Previous studies have shown the validity of this regularity for our solar system, and for some selected exoplanet systems. Here, we study all the systems which are known with four or more planets. A remarkable result is found: 63 out of 100 systems show a better agreement between the theory and observation than our solar system. We discuss the relation between the symmetry-inspired transformations and the generalized Titius–Bode (gTB) rule. It turns out that the gTB rule, which has been considered purely empirical, can be obtained from the transformations corresponding to the dynamical group of the Kepler problem.

Keywords: astronomy data analysis; celestial mechanics; planetary system evolution; exoplanet systems



Citation: Cseh, J.; Dang, P.; Szilágyi, S.; Lévai, G. Orbital Regularity of Exoplanets and the Symmetries of the Kepler Problem. *Symmetry* **2023**, *15*, 2114. <https://doi.org/10.3390/sym15122114>

Academic Editors: Carlos Frajuca, Nadja Simão Magalhães and Jerzy Kowalski-Glikman

Received: 17 October 2023

Revised: 13 November 2023

Accepted: 23 November 2023

Published: 26 November 2023



Copyright: © 2023 by the authors. Licensee MDPI, Basel, Switzerland. This article is an open access article distributed under the terms and conditions of the Creative Commons Attribution (CC BY) license (<https://creativecommons.org/licenses/by/4.0/>).

1. Introduction

The mystery of the sequence of planets in a planetary system has a long history. Kepler raised this question [1] before he found the laws of planetary motion [2,3]. His guess showed a beautiful harmony: the six planetary orbits (known at their time) are connected by the five regular polyhedra. One can say he proposed a transformation rule which can produce the distances of the planets from the Sun, if one of them is known. It turned out that this Divine Harmony did not reflect the real circumstances.

Later on, several empirical formulae were proposed; the best known one is the Titius–Bode rule [4,5]. Nevertheless, the final and completely satisfying answer is still not known. Both the physical origin of these rules and the way of their application (applying the sequence numbers to the planets) have considerable uncertainties.

In 1989, Barut proposed a symmetry-governed approach to the problem [6]. He applied a dilatation transformation, which is in line with the dynamical group of the Kepler problem. By the Kepler problem, we mean the motion of a single planet around a heavy sun. He found that the orbital parameters of the planets in our solar system follow this rule to a good approximation. In a recent work, one of us investigated if the observed data of some selected exoplanetary systems follow the symmetry-governed transformations [7]. A remarkable agreement was found.

In this paper, we study the systems of exoplanets systematically from this viewpoint. In particular, we investigate all extrasolar systems with four or more planets.

Furthermore, we discuss the relation of the empirical Titius–Bode rule and the dilatations corresponding to the dynamical group of the Kepler problem. It turns out that the generalized (two-parameter) Titius–Bode (gTB) rule [8,9] can be obtained from the transformations introduced by Barut based on the most general symmetry of the Kepler

problem. Hence, a new light is shed on the physical background of the rule, which has been considered so far completely empirical.

Some preliminary aspects of this investigations were published in [7], as mentioned above. There only six exoplanetary systems were considered, whereas here, we carry out a systematic investigation by studying all the 100 known systems with four or more planets. The connection between the (generalized) Titius–Bode rule and the transformations of the dynamical group of the Kepler problem has not been discussed in [7], nor in any other work to the best of our knowledge. Here we point out this connection, which might be worth for further attention. Since the symmetries of the Kepler problem are not very widely known, and were mentioned only briefly in [7], we present it here with some details.

In what follows, in Section 2, we consider some of the models available for the distribution of the planetary orbits, and pay special attention to Barut’s conjecture. In Section 3, we review the symmetries of the Kepler problem, which give the theoretical background for the transformations, and show some connection to the Titius–Bode rule. In Section 4, our calculations for the exoplanet systems are presented. Finally, Section 5 concludes our investigation.

The transformation rules between the planetary orbits allow, of course, predictions of missing planets [10]. The careful investigation of this problem, however, is a considerable task, and deserves a separate work; therefore, we leave it for further studies.

2. Distribution of Planetary Orbits

2.1. The Titius–Bode Rule

The best known rule to give the distribution of planetary orbits in our solar system is the Titius–Bode (TB) formula [4,5]. According to this rule, the semi-major axis of the planetary orbits is as follows:

$$R_n = d + R_0 \times b^n, \quad (1)$$

with $d = 0.4$ au, $R_0 = 0.3$ au, $b = 2$, where au stands for astronomical unit (1 au is the length of the semi-major axis of Earth’s orbit). The sequence of numbers (n) for the planets (Me: Mercury, V: Venus, E: Earth, Ma: Mars, A: Asteroids, J: Jupiter, S: Saturn, U: Uranus, N: Neptune, P: Pluto) is as follows $-\infty$: Me, 0: V, 1: E, 2: Ma, 3: A, 4: J, 5: S, 6: U, 7: P (which does not account for the orbit of Neptune). As can be seen, the numbers are not regular, and a theoretical background of this empirical formula is not really known. This original TB rule is a three-parameter formula.

Later on, a two-parameter generalized TB formula was invented [8,9]:

$$R_n = R_0 \times C^n. \quad (2)$$

This equation was used in the analysis of exoplanets, as well as simulated systems, see [11] and references therein.

In [12], the TB rule was related to the rotational and scale invariances, and it was shown that one can obtain this kind of rules from a disk model, e.g., see [13].

Further empirical formulae were also proposed in [14–16], and the significance of this kind of rules was investigated statistically by [17].

2.2. Barut’s Conjecture

Barut [6] related the sequence of planets in our solar system to the hidden symmetries of the Kepler problem. He discovered that the logarithms of the orbital velocities, periods, and distances of the planets are linear functions of the natural sequence number as follows: 1: Me, 2: V, 3: E, 4: Ma, 5: A, 6: J, 7: S, 8: U, 9: N, 10: P; a graphical demonstration is given in Figure 1.

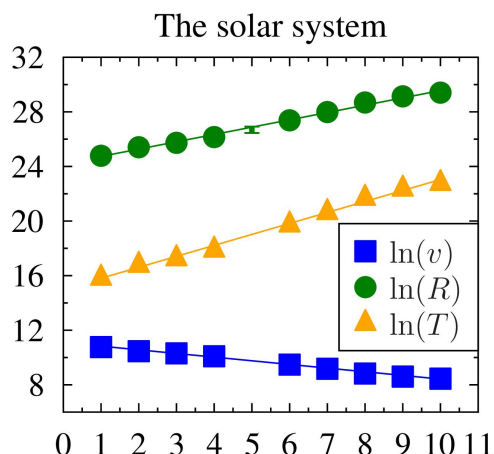


Figure 1. The logarithm of the orbital parameters—velocities (v), periods (T), and semi-major axes (R)—of planets in the solar system. The sequence of numbers is the following: 1: Mercury, 2: Venus, 3: Earth, 4: Mars, 5: Asteroids, 6: Jupiter, 7: Saturn, 8: Uranus, 9: Neptune, 10: Pluto. Since the Asteroid Belt subsumes a tremendous number of asteroids and its nature differs from that of a planet, we did not take it into account during the calculation; rather, we left an empty position, and then we demonstrate it by a segment covering a region from 2.06 au to 3.27 au. This figure resembles the original work performed by Barut [6].

It was also realized that the orbital connection emerges from a simple time-and-space dilatation:

$$t \rightarrow e^{3\lambda n} t, \quad x \rightarrow e^{2\lambda n} x, \tag{3}$$

giving the following equations:

$$\begin{aligned} \ln v_n &= \ln v_0 - \lambda n, \\ \ln R_n &= \ln R_0 + 2\lambda n, \\ \ln T_n &= \ln T_0 + 3\lambda n, \end{aligned} \tag{4}$$

where λ is a constant characteristic to the solar system (or any other system of interest), and it allows us to predict any planetary orbitals, should one of them be known beforehand.

The surprising new element of Barut’s work is that the $O(4,2)$ dynamical group of the Kepler problem [6] suggests the time–space transformation (3). Hence, Barut’s proposal gives the regularity anticipated by Kepler [1]: the planetary orbitals can be determined from the first one in a simple manner, and the relationship has a theoretical connection to the hidden symmetry of the Kepler problem.

The time and space dilatation of Equation (3) provides us with the generalized TB rule:

$$R_n = R_0(e^{2\lambda})^n, \quad T_n = T_0(e^{3\lambda})^n, \tag{5}$$

which contains Kepler’s third law of planetary motion. Thus, the (generalized) Titius–Bode rule, which was considered beforehand as an empirical rule without real theoretical background, seems to have a close connection with the dynamical algebra of the Kepler problem.

In the next section, we review the hidden symmetries of the Kepler problem, because their role can shed a new light on the regularity of planetary orbits.

3. Symmetries of the Kepler Problem

3.1. Geometrical Symmetry

The obvious symmetry of the Kepler problem is that of the rotation in three-dimensional space: $O(3)$. The gravitational force depends only on the distance between the Sun and the considered planet; it does not depend on the direction (the transformations of the $O(3)$ group leave invariant the $x_1^2 + x_2^2 + x_3^2$ quadratic form). Therefore, the problem has

rotational invariance. As a consequence, the angular momentum is conserved, and its vector, as follows:

$$\vec{L} = \vec{r} \times \vec{p} \tag{6}$$

is a constant of the motion. The three components of the angular momentum close under the Poisson bracket:

$$\{L_i, L_j\} = \epsilon_{ijk}L_k, \tag{7}$$

that is, they form a Lie-algebra (here, the Levi-Civita symbol $\epsilon_{ijk} = 1$ for (1,2,3), (2,3,1), (3,1,2); $\epsilon_{ijk} = -1$ for (1,3,2), (2,1,3), (3,2,1); $\epsilon_{ijk} = 0$ for $i = j$, or $j = k$, or $k = i$). The elements of the algebra generate the Lie-group O(3).

The energy of the system is as follows:

$$H = T + V = \frac{p^2}{2m} - \frac{c}{r}, \tag{8}$$

where $c = \gamma Mm$, M and m are the masses of the Sun and the planet, respectively, while γ is the gravitational constant (the actual value of H will be denoted later on by E). The Poisson bracket of the energy (H) with all the components of the angular momentum (L_i) is zero:

$$\{L_i, H\} = 0, \quad i = 1, 2, 3. \tag{9}$$

This symmetry is called *geometrical symmetry*, because it transforms the geometrical variables—space coordinates—into each other (and does not mix them with others, e.g., with the momenta). Not only does it leave the total Hamiltonian (H) unchanged, but its kinetic (T) and potential (V) parts are also invariant:

$$\{L_i, T\} = 0, \quad \{L_i, V\} = 0, \quad i = 1, 2, 3. \tag{10}$$

3.2. Dynamical Symmetry

In addition to the obvious symmetry of the three-dimensional rotations, the Kepler problem has a hidden symmetry (in what follows, we consider the bound state problem, i.e., the energy is negative and the orbit is an ellipse). Not only the angular momentum, but another vector, called the Laplace, or Runge–Lenz vector, is also a constant of motion:

$$\vec{\epsilon} = \frac{\vec{r}}{r} + \frac{\vec{L} \times \vec{p}}{cm}. \tag{11}$$

This vector is in the plane of the orbit, and it is perpendicular to the angular momentum. Since it is conserved, the following equations:

$$\{\epsilon_i, H\} = 0, \quad i = 1, 2, 3 \tag{12}$$

are also fulfilled. The two-times-three components of the angular momentum and the Runge–Lenz vector close under the Poisson bracket. It is more convenient to express their relations with the following vectors:

$$\vec{A} = c \left(\frac{m}{2|E|} \right)^{\frac{1}{2}} \vec{\epsilon} \tag{13}$$

$$\{L_i, A_j\} = \epsilon_{ijk}A_k, \tag{14}$$

$$\{A_i, A_j\} = \epsilon_{ijk}L_k. \tag{15}$$

Thus, they form a Lie-algebra, and the elements of this algebra generate the O(4) group. The transformations of the O(4) leave invariant the $x_1^2 + x_2^2 + x_3^2 + x_4^2$ quadratic form [18]. The hidden symmetry of the Kepler problem is, therefore, the invariance with respect to

the rotations in a four-dimensional space, which contains, of course, the three-dimensional rotations as a subgroup: $O(4) \supset O(3)$. In contrast with the $O(3)$ transformations, nonetheless, not all the $O(4)$ counterparts preserve the kinetic and the potential energy separately, but the total energy is always conserved. The $O(4)$ symmetry is characteristic for the central $1/r$ potential, and for this reason, it is termed as *dynamical symmetry*.

However, what is the four-dimensional space in which the transformations of $O(4)$ act? Interestingly enough, this question was not answered until the late 1960s.

The essential role of the $O(4)$ symmetry in the Kepler problem was realized in the 1930s. Inspired by the degeneracy of the energy levels of the Hydrogen atom, Fock found a transformation [19] between its wave functions and the four-dimensional hyperspherical harmonics Y_{nlm} . He used a stereographic projection between the three-dimensional space and the four-dimensional sphere, and while it was not really considered as “uncovering” the hidden symmetry (rather producing it), it elucidated the degeneracy. Then, Bargmann gave a Lie-algebraic treatment of $O(4)$ without projections [20].

The coordinate space of the $O(4)$ transformations was constructed by Györgyi, who gave a detailed four-dimensional description of the problem [21,22]. Another four-dimensional treatment is presented by [23] in the language of the more recent (geometrized) Hamiltonian mechanics.

Here, we recall the basic concepts of the description of Györgyi because it is less well-known, though it was the first four-dimensional treatment to deliver very interesting results.

Let us define p_0 and r_0 by the following equation:

$$E = -\frac{p_0^2}{2m} = -\frac{c}{2r_0}. \quad (16)$$

With:

$$\vec{e} = \frac{cm}{p_0^2} \vec{e} \quad (17)$$

one can introduce the following four-dimensional space and momentum vectors:

$$\vec{\pi} = \frac{2p_0^2}{p_0^2 + p^2} \vec{p}, \quad \pi_4 = \frac{p_0^2 - p^2}{p_0^2 + p^2} p_0; \quad (18)$$

$$\vec{\rho} = \vec{r} - \vec{e}, \quad \rho_4 = -[r_0^2 - (\vec{r} - \vec{e})^2]^{\frac{1}{2}}. \quad (19)$$

The six constants of motion can be arranged in a second rank four-dimensional antisymmetric tensor $F_{\alpha,\beta}$. It is obtained from the space and momentum vectors as follows:

$$F_{\alpha,\beta} = \rho_\alpha \pi_\beta - \rho_\beta \pi_\alpha. \quad (20)$$

The energy is:

$$H = -\frac{c^2 m}{F_{\alpha,\beta} F_{\alpha,\beta}} \quad (21)$$

For the indices with double appearance, a summation is understood from 1 to 4. The orthogonal transformations of the four-dimensional space leave the energy invariant, and if π_α, ρ_α are the vectors of a Kepler orbit, then the transformed $\pi'_\alpha, \rho'_\alpha$ vectors correspond to a possible Kepler orbit of the same energy.

It is useful to also introduce the invariant time parameter, as follows:

$$d\tau = \frac{p_0^2 + p^2}{2p^2} dt. \quad (22)$$

Then, the equation of motions have the following simple and symmetric form:

$$\frac{d\rho_\alpha}{d\tau} = \frac{1}{m} \pi_\alpha, \quad (23)$$

$$\frac{d\pi_\alpha}{d\tau} = -\frac{p_0^2}{mr_0} \frac{\rho_\alpha}{r_0}. \quad (24)$$

These equations depict an inertial motion along the main circles of a sphere in the four-dimensional space. In other words, the Keplerian orbits in this hyperspace are perfect, i.e., they are circles. In addition, the problem is relegated to a kinematic one, wherein the gravitational force occurring in the three-dimensional framework vanishes and the inertial motion is constrained to a hypersphere. This feature resembles somewhat that of the general relativity.

We note here that none of the six constants of motion (X_j) described above have explicit time dependence:

$$\frac{\partial X_j}{\partial t} = \{X_j, E\} = 0. \quad (25)$$

3.3. Dynamical Algebras

The symmetry groups transform the states of the same energy into each other. We may look for a larger group which connects all the states, not only the ones with a specific energy. This group is called a dynamical group, and its algebra is dynamical algebra.

The concept of the dynamical algebra was raised in quantum mechanical problems [24], and for a while, it was applied only there. It is an algebra “that can yield the energy spectrum and the degeneracies of the levels, and that contains a set of operators that determine the transition probabilities between states” [18]. A well-known example is the $U(6)$ dynamical algebra of the collective motion in atomic nuclei [25]. The nuclei can rotate and vibrate, and their complete rotational–vibrational spectrum, including the energy levels, their degeneracy, and the electromagnetic transitions between them, can be obtained within a single irreducible representation of the $U(6)$ algebra.

For some time, it was not clear how the concept of the dynamical algebra could be interpreted in classical mechanical systems. In the quantum mechanical application of the group theory, the representations play a crucial role, but in classical mechanics only the defining representation occurs.

Nowadays, an interpretation of the dynamical algebra in classical mechanics is available. In fact, a parallel definition can be applied in classical and quantum mechanics. We summarize the basic concepts following the work in [26], and we refer to that paper concerning previous studies, too.

The symmetry algebra is spanned by the constants of motion of the problem, as mentioned in the previous subsection. This definition is applicable both in classical and in quantum physics. Those constants of motion have no explicit time dependence. There are, nevertheless, constants of motion with explicit time dependence as well. In classical mechanics, the total time derivative (of f) is given by the partial derivative and the Poisson bracket:

$$\frac{df}{dt} = \frac{\partial f}{\partial t} + \{E, f\}. \quad (26)$$

Hence, a physical quantity can be constant even if it has an explicit time dependence (i.e., nonzero partial time derivative).

The constants of motion, including the ones with explicit time dependence, span the dynamical algebra. This set contains, of course, the elements of the symmetry algebra, too, and thus, the symmetry algebra is a subalgebra of the dynamical algebra.

The parallel interpretation of the dynamical and symmetry algebras in the classical and quantum treatment is based on the following correspondence. First, the Poisson bracket of the dynamical variables A and B corresponds to the commutator of the \hat{A} and \hat{B} operators:

$$\{A, B\} \rightarrow -i[\hat{A}, \hat{B}] \quad (27)$$

where $\hbar = 1$ is assumed. Second, the equation of motion of a physical operator in the Heisenberg picture is formally identical with that of the corresponding function in classical mechanics.

3.4. $O(4,2)$ and the Kepler Problem

The transformations of the four-plus-two dimensional $O(4,2)$ orthogonal group leave invariant the $x_1^2 + x_2^2 + x_3^2 + x_4^2 - x_5^2 - x_6^2$ quadratic form. Its first physical application was a global (or external) space–time transformation belonging the conformal group—a specific nonlinear realization of the dynamical group $O(4,2)$. In particular, the four Maxwell equations are invariant with respect to the conformal transformations of this group. The construction of the algebra that spans the conformal group is as follows. First, it subsumes the six elements of the $O(3,1)$ Lorentz algebra and the four generators of transformation belonging to the Poincare group (also known as the inhomogeneous Lorentz group $IO(3,1)$). Next, to ensure the existence of inverted group elements, the addition of five new generators is necessary. One of them is a scalar, which is the following dilatation:

$$x'_\mu = \zeta x_\mu, \quad (28)$$

whereas the other four constitute a 4-vector.

The group $O(4,2)$ also serves as the dynamical group of a rest frame system whose dynamics depends on some internal degrees of freedom. This resembles the problem of finding the dynamical algebra for studying the Hydrogen atom in quantum mechanics. The Hamiltonian \hat{H} , the angular momentum \hat{L}^2 , and the projection on the z -axis \hat{L}_z form a complete set of observables; three quantum numbers $|nlm\rangle$ are used to label different states. The algebra that we are looking for must contain the $O(4)$ symmetry algebra as a subalgebra, and also consist of raising and lowering operators that change n and l [18] from one to others. Furthermore, the elements of the $O(4,1)$ algebra is required to incorporate states with different energy; and the $O(4,2)$ generators are needed to include continuum states and transition operators.

In [27], the authors presented the unification of the external and internal $O(4,2)$ groups with a description of a two-body system in a six-dimensional space. The equations of motion remain unchanged under rotations in the six-dimensional space, i.e., they are conformally invariant in the four-dimensional Minkowski space. The total algebra is obtained via the direct sum of the conformal algebra in the space of external position coordinates and the dynamical algebra in the space of the internal position coordinates. This astonishing and intriguing interconnection between the two roles of the $O(4,2)$ plays a key role behind the space–time transformation (3), though the authors did not consider it a “completely conclusive and final answer” [27].

The considerations reviewed briefly in this section give the theoretical background of Barut’s proposal [6] mentioned beforehand. In the following section, we test this proposal with respect to new data.

4. Exoplanetary Systems

4.1. Data Collection and Analysis

In [7], only a few quintuple-planet or bigger systems were taken into consideration. Here, our exploration covers as many cases as possible by looking at all exoplanetary systems having four or more planets.

In order to execute linear regression based on Barut’s transformation, orbital periods (T), semi-major axes (R), and the average orbital velocities (v) of exoplanets needed gathering first. These quantities are not independent, of course. The orbital period and the semi-major axis are related by Kepler’s third law of planetary motion. Most exoplanets have been discovered using indirect methods, each of which determines the orbital parameters and uncertainties of the planets with different sensitivities. Among the parameters, the period (and then the semi-major axis) can be considered with the least uncertainty. On the other hand, the velocity is not directly detectable; rather, it is obtained from the

observed quantities, as discussed below. Nevertheless, we consider all these three characteristics of the orbital motion (as it was suggested by Barut) in order to make the comparison between the observation and theory as complete, as possible. The procedure we followed is summarized here.

1. We collected astronomical data from four sources: NASA Exoplanet Archive [28], Open Exoplanet Catalogue [29], The Extrasolar Planets Encyclopaedia [30], and Exoplanets Data Explorer [31,32]. We note that system HIP 41378 was a special case—in fact, in [29] only HIP 41378 g was available, but in [30] HIP 41378 b,c,d,e,f were given, wherefore the complete dataset was taken from a paper [33].
2. Data were then converted to SI units. The orbital periods, T , were expressed in seconds (1 day = 86,400 s). Likewise, the lengths of semi-major axes, R , were converted from the astronomical unit to meter (1 au = 149,597,870,691 m). We note that in each system, planets are indexed by b, c, d, e, etc. according to the order of discoveries, and thus, they were reorganized in the ascending order of the semi-major axes. Since the average velocities were not available, we determined them by the following relationship [34]:

$$v = \frac{2\pi R}{T} \left(1 - \frac{1}{4}\varepsilon^2 - \frac{3}{64}\varepsilon^4 - \frac{5}{256}\varepsilon^6 - \frac{175}{16,384}\varepsilon^8 \right), \quad (29)$$

where ε is the eccentricity of the elliptical orbit—which is the modulus of the eccentricity vector introduced in Equation (11). Below, we briefly present two aspects on the collection of eccentricities that are worth noting.

3. Unfortunately, some systems did not have a complete dataset, i.e., orbital period, or semi-major axis, or eccentricity was not available. For example, all six planets of TOI-1136 in [28,30] had data of orbital periods and eccentricities, but no semi-major axes, and as a result, not enough data to calculate the average speeds. Nonetheless, these cases were also considered if the number of planets with complete published data was not less than four. In these cases, the flawed planet was simply excluded and left an empty space. Yet, when plotting all the data, we observed merely moderate deviation from the fitting line of the rest (see Appendix A).
4. Combining four databases led to redundancy and overlap of information—indeed, some exoplanetary systems appeared in more than one source with different details (even the number of planets), such as HD 10180, GJ 667 C, Kepler-444. In such cases, we chose the complete dataset. When the same number of exoplanets were listed in all data sources without any missing information, we preferred NASA Exoplanet Archive [28] (as it is the most well-known data compilation).

Following this process, we found 100 exoplanetary systems altogether: 64 quadruple-planet, 21 quintuple-planet, 9 sextuple-planet, 4 septuple-planet, 1 octuple-planet, and 1 nonuple-planet.

As aforementioned, we would like to reserve a small discussion on the collection of orbital eccentricities. First, there are some planets whose eccentricity is provided ambiguously in the data source. To be specific, it is given less than a number in lieu of a particular value; in this case, our calculation simply takes the limit given in the database. This does not affect the final conclusion significantly: as an example, it can be shown from Equation (29) that in the second-order approximation, if the eccentricity is said to be less than 0.3, the velocity changes merely 4.6% when the real value differs from 0.3 by 100% (i.e., we have a circular orbit), implying that the fitting will not be so different. Second, we investigate several systems in which all planets move on circular orbits ($\varepsilon = 0$). This is completely justified on the grounds that: (i) high multiplicity is often associated with low eccentricity (or nearly circular orbit) [35] and (ii) changes in the eccentric value results in inconsiderable change in the value of velocity, and consequently, the fitting, as we have just showed.

4.2. Fitting Barut’s Equations

We apply here the common least square method simultaneously on Equation (4) to find the four unknowns, namely λ , v_0 , R_0 , and T_0 . Here, “simultaneously” means that those three equations are fitted at the same time—having a joint λ , not one by one. In particular, for a system with n planets, the following function is minimized:

$$F = \sum_{i=1}^n [(\ln v_i^o - \ln v_i^f)^2 + (\ln R_i^o - \ln R_i^f)^2 + (\ln T_i^o - \ln T_i^f)^2], \tag{30}$$

where o and f refer to observational data and fitted values, respectively. Thereby, we also characterize the goodness of the fitting by introducing the standard error:

$$\sigma = \sqrt{\frac{F}{3n}}. \tag{31}$$

One may question what if we fitted those linear equations independently—the answer is that the results are essentially not different. As we have shown previously, R , v , and T are correlated, implying that fitting any one of them separately leads to basically the same λ . For example, the difference between λ obtained from the fitting of T only and λ values of the simultaneous fitting (displayed in Table A1) appears in the fourth or fifth significant digit in the majority (75%) of the cases.

Figure 2 shows some examples of the fitting procedure, and the complete results are presented in Table A1 and Appendix A.

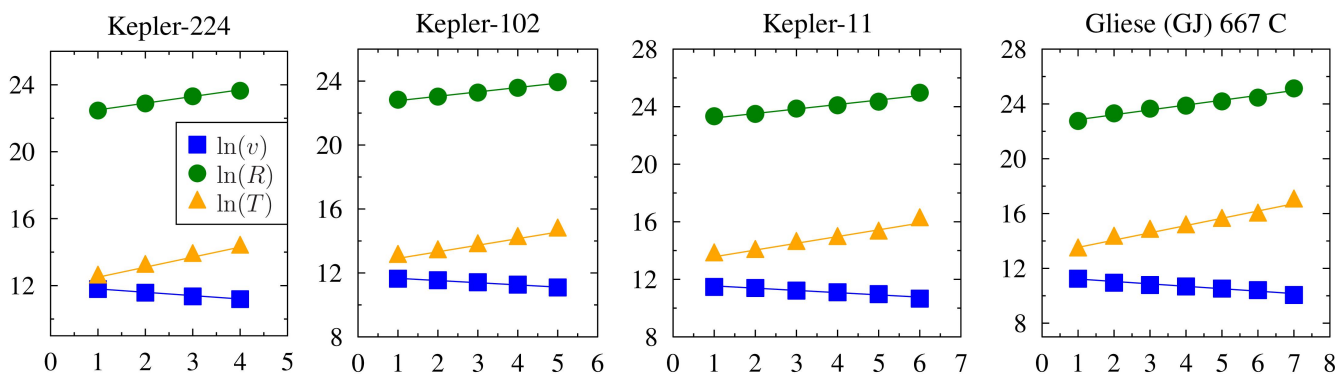


Figure 2. Some exoplanetary systems studied by Barut’s transformation (4). The values of the parameters λ , v_0 , R_0 , T_0 , and the standard error σ can be found in Table A1.

It is worth mentioning that the solar system is a special case, see Figure 1, owing to two reasons. First, the Asteroid Belt—due to its huge number of asteroids—was excluded from the fitting process, yet we plot its range of semi-major axes together with the other planets in the system and it does not show any notable disagreement. Second, despite being a dwarf planet and not possessing the usual orbital characteristics of the other planets, Pluto was taken into the regression to honor Barut’s original work. Having said that, we also try to see the effect when removing Pluto—indeed, if it were not considered, the standard error would drop roughly by 10.3% from 0.1344 to 0.1206.

Statistics of the values of the parameter λ , the standard error σ , and the constants v_0 , R_0 , T_0 are shown by histograms (see Figures 3a,b and 4a–c). We note that in these statistics, we also took the solar system into account.

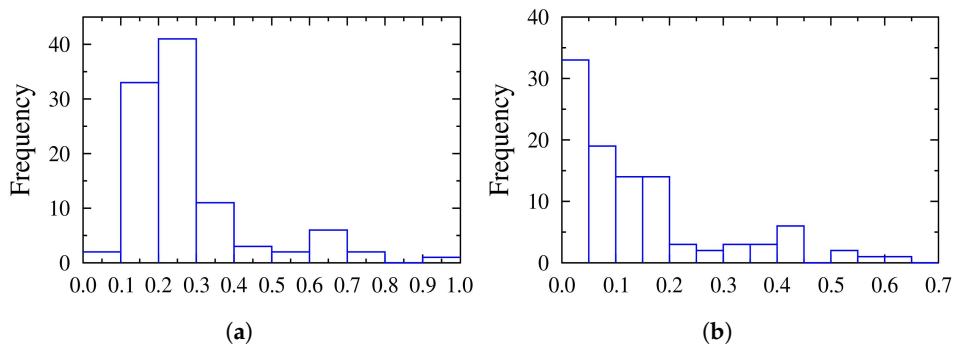


Figure 3. Statistics of the characteristic parameter λ and the standard error of the linear fitting. Details are given in Table A1. (a) λ ; (b) σ calculated by Equation (31).

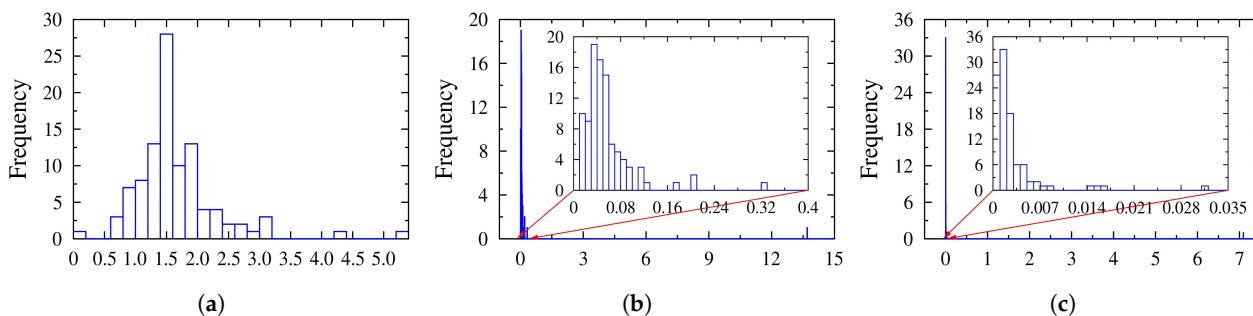


Figure 4. Statistics of the parameters v_0, R_0, T_0 obtained from the linear fitting. Details are given in Table A1. (a) $v_0(10^5 \text{ m/s})$. (b) $R_0(10^{11} \text{ m})$. (c) $T_0(10^8 \text{ s})$.

It can be seen that λ is lower than 1.0 and the range between 0.1 and 0.3 dominates, accounting for roughly 73% of the whole sample, which is a very surprising trait because there seems to be no constraint on the values of λ in the time–space transformation (see Equations (3) and (4)). Furthermore, a closer look at Figure 3a,b also reveals that their distributions seemingly follow an expected trend up to some points; thereafter, however, some unusual local peaks show up. To be specific, there are nine systems having $\lambda > 0.6$ and eleven ones having $\sigma > 0.4$, where the local peaks start to develop; it turns out that there are six systems possessing both these features, namely GJ 221, HD 1461, HD 160691, mu Ara, Upsilon Andromedae, WASP-47. Looking at their corresponding plots in Appendix A, one sees that these systems display the most “irregular” look, too. It implies that large λ may be associated with large σ . Inserting a planet into the system would lower σ (better fitting), but also λ . Therefore, perhaps these systems are those containing undetected planets. Were this the case, the unexpected peaks would probably disappear in the distributions and their tail would behave more like that of an ordinary distribution. A deeper discussion of this topic is beyond the scope of the present paper. Moreover, in contrast with most of the cases, which have been detected by the transition method, the systems forming the tail of the two distributions were detected by other methods, which may also be responsible for their different appearance.

In the case of R_0 and T_0 (Figure 4b,c), one can witness that there is one system which differs significantly from the others—in fact, it is HR 8799 having four planets at the time of data collection, and thus, we anticipate that it may have more planet(s) and when those uncovered are found, its parameters will come closer or even fall into the popular ranges. Indeed, there have been numerous interests poured into this exoplanet system to seek a possible candidate for the fifth planet, e.g., Goździewski and Migaszewski predicted a planet at 7.5 au or 9.7 au from its host star [36]. In a recent work, Thompson et al. [37] performed a deep orbital search and suggested a potential innermost planet with a semi-major axis of 4.3250 au for the coplanar case and 4.5103 au for the noncoplanar case. Fitting this system again shows that the coplanar candidate brings this system closer to the rest—to

be specific, the new $R_0 = 5.8157 \times 10^{11}$ m and $T_0 = 2.3404 \times 10^8$ s are about 58% and 67% smaller than the current values with only four planets.

Now, it is rational to conclude that the observed data and the symmetry-inspired rule agree with each other, since the standard error is always less than 1.0 as shown in Figure 3b (which is insignificant compared to the orders of magnitude of the data). Hence, this systematic investigation over 100 systems suggests that the orbital regularity in planetary systems (both solar and extrasolar) stem from the time–space dilation emerging from the dynamical group $O(4,2)$ of the Kepler problem.

5. Summary and Conclusions

In this work, we have investigated to what extent the exoplanet systems can be described by the symmetry-inspired rules of Equation (4), as suggested by Barut [6]. The question goes back to the early works by Kepler, searching for a transformation, which takes us from the orbit of one planet to those of the other ones. The applicability of Barut's conjecture was addressed beforehand only for our solar system by [6], and for a few selected systems of exoplanets by [7]. Here, we studied it systematically, including all the systems known with four or more planets, therefore, we investigated 100 planetary systems; in particular, the star-distances, the periods, and the average velocities were considered.

The important new feature of Barut's conjecture is that it is related to the (most general) symmetry of the Kepler problem. In particular, it applies dilatation, which is in line with the dynamical group of the problem. This situation is very different from those of the empirical Titius–Bode type rules. The transformations—Equations (3)–(5)—which take the planetary orbits into each other provide us with the generalized (two-parameter) Titius–Bode rule, Equation (2). Therefore, it sheds a new light on the theoretical background of this successful empirical rule. A further novel characteristics of the present approach is that it applies the concept of the dynamical group in celestial mechanics. Dynamical groups and algebras were introduced in quantum mechanics, and their overwhelming use falls to that territory.

In general, the symmetry-governed transformations describe the observed data of the exo-planetary systems to a good approximation. In total, 63 systems out of the 100 show a better agreement between the data and the theoretically calculated values than our solar system. When the observed patterns differ from geometric progression predicted by Barut's rule, one might think that the reasons are extraordinary circumstances, e.g., due to missing planet(s). An unusually large standard error may be a sign of it.

The present study may contribute to the understanding of the physical background of the Titius–Bode rule, but it also raises several questions. One of the most exciting ones is: how the symmetry-related simple sequence of the one-body problem originates from the complex many-body (gas or fluid) dynamics of the planetary evolution.

Author Contributions: Conceptualization, J.C., S.S. and G.L.; methodology, all; Fortran program for fitting data, J.C.; data collection and analysis, P.D., G.L. and S.S.; writing—original draft preparation, J.C. and P.D.; writing—review and editing, all; visualization, P.D. All authors have read and agreed to the published version of the manuscript.

Funding: This work was funded by the National Research, Development, and Innovation Fund of Hungary, financed under the K18 funding scheme with project no. K 128729. In addition, financial support from the TalentUD program of the University of Debrecen, Hungary is appreciated.

Data Availability Statement: Data produced in this article can be found at https://drive.google.com/drive/folders/12Yy5iF6hNgR5taHjyEUVPACETk7rP_8f?usp=sharing (accessed on 9 January 2023).

Acknowledgments: Useful discussions with Géza Györgyi Jr. are kindly acknowledged.

Conflicts of Interest: The authors declare no conflict of interest.

Abbreviations

The following abbreviations are used in this manuscript:

- TB rule the Titius–Bode rule
- gTB rule the generalized Titius–Bode rule

Appendix A. Results of the Fitting and Graphical Illustration of Barut’s Rule

Table A1. Results of the fitting process to exoplanetary systems. $\ln v_0$, $\ln R_0$ and $\ln T_0$ are the intercepts in Equation (4), while λ is the slope characteristic for each system; the standard error evaluated by Equation (31) denotes the quality of the linear regression. System names in parentheses are alternative names of the systems. “Nump.” means the number of planets inside the corresponding system.

System Name	Nump.	v_0 (m/s)	R_0 (m)	T_0 (s)	λ	σ
DMPP-1 (HD 38677)	4	1.949×10^5	4.215×10^9	1.357×10^5	1.923×10^{-1}	1.280×10^{-1}
GJ 221 (BD-06 1339)	4	3.105×10^5	9.137×10^8	1.837×10^4	6.482×10^{-1}	4.417×10^{-1}
GJ 273	4	1.445×10^5	1.603×10^9	6.499×10^4	6.072×10^{-1}	3.931×10^{-1}
GJ 3293	4	8.446×10^4	7.743×10^9	5.732×10^5	2.373×10^{-1}	7.176×10^{-2}
GJ 676 A (Gliese 676 A)	4	3.168×10^5	8.023×10^8	1.565×10^4	9.394×10^{-1}	1.635×10^{-1}
GJ 876	4	1.470×10^5	1.946×10^9	8.262×10^4	4.394×10^{-1}	4.015×10^{-1}
HD 141399	4	7.742×10^4	2.080×10^{10}	1.678×10^6	4.494×10^{-1}	1.701×10^{-1}
HD 1461	4	3.177×10^5	1.320×10^9	2.590×10^4	7.932×10^{-1}	4.105×10^{-1}
HD 160691	4	1.495×10^5	5.742×10^9	2.406×10^5	6.216×10^{-1}	4.352×10^{-1}
HD 164922	4	1.564×10^5	5.001×10^9	2.006×10^5	4.770×10^{-1}	3.594×10^{-1}
HD 20781	4	7.409×10^4	1.740×10^{10}	1.467×10^6	1.437×10^{-1}	1.717×10^{-1}
HD 20794	4	9.004×10^4	1.177×10^{10}	8.175×10^5	2.369×10^{-1}	5.902×10^{-2}
HD 215152	4	1.313×10^5	5.713×10^9	2.686×10^5	1.604×10^{-1}	1.115×10^{-1}
HD 3167	4	2.983×10^5	1.166×10^9	2.358×10^4	5.105×10^{-1}	1.866×10^{-1}
HR 8799	4	1.212×10^4	1.369×10^{12}	7.094×10^8	2.534×10^{-1}	4.416×10^{-2}
K2-285	4	1.918×10^5	5.759×10^9	1.885×10^5	1.709×10^{-1}	1.869×10^{-1}
K2-32	4	1.511×10^5	4.815×10^9	2.000×10^5	2.264×10^{-1}	6.745×10^{-2}
K2-72	4	9.400×10^4	4.099×10^9	2.732×10^5	1.689×10^{-1}	5.017×10^{-2}
Kepler-106	4	1.390×10^5	6.558×10^9	2.966×10^5	2.151×10^{-1}	3.916×10^{-2}
Kepler-107	4	1.835×10^5	4.635×10^9	1.586×10^5	1.695×10^{-1}	3.354×10^{-2}
Kepler-132	4	1.865×10^5	3.845×10^9	1.294×10^5	3.218×10^{-1}	3.192×10^{-1}
Kepler-1388	4	1.228×10^5	5.343×10^9	2.735×10^5	2.094×10^{-1}	4.573×10^{-2}
Kepler-1542	4	1.567×10^5	5.062×10^9	2.030×10^5	8.132×10^{-2}	2.723×10^{-2}
Kepler-167	4	2.738×10^5	1.375×10^9	3.154×10^4	5.858×10^{-1}	6.336×10^{-1}
Kepler-172	4	1.984×10^5	3.417×10^9	1.082×10^5	2.758×10^{-1}	1.780×10^{-2}
Kepler-176	4	1.445×10^5	5.423×10^9	2.359×10^5	2.469×10^{-1}	3.488×10^{-2}
Kepler-197	4	1.341×10^5	6.637×10^9	3.080×10^5	1.652×10^{-1}	3.266×10^{-2}
Kepler-208	4	1.581×10^5	6.232×10^9	2.477×10^5	1.479×10^{-1}	3.640×10^{-2}
Kepler-215	4	1.256×10^5	7.506×10^9	3.755×10^5	2.232×10^{-1}	6.506×10^{-2}
Kepler-220	4	1.564×10^5	3.974×10^9	1.597×10^5	2.777×10^{-1}	9.605×10^{-2}
Kepler-221	4	1.749×10^5	3.742×10^9	1.343×10^5	2.073×10^{-1}	2.380×10^{-2}
Kepler-223	4	1.247×10^5	8.969×10^9	4.509×10^5	1.118×10^{-1}	1.893×10^{-2}
Kepler-224	4	1.591×10^5	3.868×10^9	1.528×10^5	1.999×10^{-1}	2.858×10^{-2}
Kepler-235	4	1.618×10^5	3.058×10^9	1.188×10^5	2.940×10^{-1}	1.633×10^{-2}
Kepler-24	4	1.518×10^5	5.799×10^9	2.404×10^5	1.636×10^{-1}	4.655×10^{-2}
Kepler-245	4	1.767×10^5	3.553×10^9	1.264×10^5	2.705×10^{-1}	2.291×10^{-2}
Kepler-251	4	1.634×10^5	4.379×10^9	1.682×10^5	3.237×10^{-1}	9.962×10^{-2}
Kepler-256	4	2.217×10^5	2.781×10^9	7.875×10^4	2.069×10^{-1}	3.291×10^{-2}
Kepler-26	4	1.468×10^5	3.661×10^9	1.567×10^5	2.696×10^{-1}	1.335×10^{-1}
Kepler-265	4	1.383×10^5	6.519×10^9	2.963×10^5	2.604×10^{-1}	9.174×10^{-2}
Kepler-282	4	1.157×10^5	8.180×10^9	4.442×10^5	1.762×10^{-1}	3.990×10^{-2}
Kepler-286	4	2.359×10^5	1.999×10^9	5.332×10^4	2.971×10^{-1}	1.938×10^{-1}
Kepler-299	4	1.962×10^5	3.356×10^9	1.074×10^5	2.830×10^{-1}	2.327×10^{-2}

Table A1. Cont.

System Name	Nump.	v_0 (m/s)	R_0 (m)	T_0 (s)	λ	σ
Kepler-304	4	2.010×10^5	2.422×10^9	7.574×10^4	2.021×10^{-1}	4.848×10^{-2}
Kepler-305	4	1.634×10^5	4.120×10^9	1.584×10^5	1.792×10^{-1}	4.500×10^{-2}
Kepler-306	4	1.586×10^5	4.066×10^9	1.611×10^5	2.559×10^{-1}	9.583×10^{-2}
Kepler-324	4	1.618×10^5	4.107×10^9	1.597×10^5	2.510×10^{-1}	1.005×10^{-1}
Kepler-338	4	1.282×10^5	9.122×10^9	4.473×10^5	1.754×10^{-1}	4.113×10^{-2}
Kepler-341	4	1.654×10^5	5.133×10^9	1.950×10^5	2.513×10^{-1}	1.301×10^{-1}
Kepler-342	4	2.262×10^5	3.176×10^9	8.826×10^4	3.358×10^{-1}	3.489×10^{-1}
Kepler-37	4	9.437×10^4	1.120×10^{10}	7.449×10^5	1.552×10^{-1}	5.788×10^{-2}
Kepler-402	4	1.533×10^5	6.257×10^9	2.565×10^5	1.154×10^{-1}	3.488×10^{-2}
Kepler-411	4	1.943×10^5	2.950×10^9	9.503×10^4	3.430×10^{-1}	1.168×10^{-1}
Kepler-49	4	1.505×10^5	3.319×10^9	1.386×10^5	2.115×10^{-1}	1.055×10^{-1}
Kepler-758	4	1.457×10^5	6.024×10^9	2.599×10^5	1.590×10^{-1}	2.345×10^{-2}
Kepler-79	4	1.128×10^5	1.217×10^{10}	6.774×10^5	2.007×10^{-1}	4.907×10^{-2}
Kepler-85	4	1.138×10^5	9.122×10^9	5.038×10^5	1.235×10^{-1}	1.384×10^{-2}
KOI-94 (Kepler-89)	4	1.923×10^5	4.431×10^9	1.425×10^5	2.923×10^{-1}	4.368×10^{-2}
L 98-59	4	1.309×10^5	2.172×10^9	1.041×10^5	1.977×10^{-1}	3.227×10^{-2}
mu Ara	4	1.579×10^5	5.713×10^9	2.264×10^5	6.322×10^{-1}	4.251×10^{-1}
TOI-1246	4	1.699×10^5	3.966×10^9	1.467×10^5	2.560×10^{-1}	1.245×10^{-1}
Upsilon Andromedae	4	2.206×10^5	3.532×10^9	9.991×10^4	7.283×10^{-1}	5.336×10^{-1}
V1298 Tau	4	1.357×10^5	7.255×10^9	3.219×10^5	2.215×10^{-1}	9.622×10^{-2}
WASP-47	4	5.291×10^5	4.837×10^8	5.708×10^3	6.879×10^{-1}	5.710×10^{-1}
55 Cnc	5	4.217×10^5	6.742×10^8	1.005×10^4	6.915×10^{-1}	3.393×10^{-1}
Gliese 163 (GJ 163)	5	1.062×10^5	4.562×10^9	2.700×10^5	3.702×10^{-1}	1.549×10^{-1}
HD 108236	5	1.511×10^5	4.902×10^9	2.038×10^5	1.752×10^{-1}	8.339×10^{-2}
HD 23472	5	1.337×10^5	4.967×10^9	2.333×10^5	1.611×10^{-1}	5.310×10^{-2}
Kepler-102	5	1.338×10^5	5.952×10^9	2.793×10^5	1.373×10^{-1}	4.740×10^{-2}
Kepler-122	5	1.404×10^5	7.112×10^9	3.184×10^5	1.888×10^{-1}	6.772×10^{-2}
Kepler-150	5	1.763×10^5	4.074×10^9	1.451×10^5	2.372×10^{-1}	4.817×10^{-2}
Kepler-154	5	1.564×10^5	4.982×10^9	2.002×10^5	2.247×10^{-1}	8.226×10^{-2}
Kepler-169	5	1.841×10^5	3.189×10^9	1.089×10^5	2.457×10^{-1}	2.835×10^{-1}
Kepler-186	5	1.487×10^5	2.871×10^9	1.212×10^5	2.715×10^{-1}	2.331×10^{-1}
Kepler-238	5	2.124×10^5	3.346×10^9	9.891×10^4	2.565×10^{-1}	8.839×10^{-2}
Kepler-292	5	1.804×10^5	3.496×10^9	1.218×10^5	1.782×10^{-1}	3.967×10^{-2}
Kepler-296	5	1.143×10^5	5.316×10^9	2.841×10^5	1.970×10^{-1}	1.317×10^{-2}
Kepler-32	5	2.421×10^5	1.440×10^9	3.738×10^4	2.672×10^{-1}	1.778×10^{-1}
Kepler-33	5	1.425×10^5	8.446×10^9	3.725×10^5	1.614×10^{-1}	1.145×10^{-1}
Kepler-444	5	1.355×10^5	5.290×10^9	2.423×10^5	8.416×10^{-2}	1.438×10^{-2}
Kepler-55	5	1.855×10^5	2.637×10^9	8.932×10^4	2.567×10^{-1}	8.517×10^{-2}
Kepler-62	5	1.576×10^5	3.657×10^9	1.452×10^5	3.325×10^{-1}	2.326×10^{-1}
Kepler-82	5	1.994×10^5	3.076×10^9	9.686×10^4	3.026×10^{-1}	1.992×10^{-1}
Kepler-84	5	1.594×10^5	5.364×10^9	2.117×10^5	1.954×10^{-1}	5.348×10^{-2}
TOI-561	5	2.710×10^5	1.427×10^9	3.306×10^4	3.724×10^{-1}	5.045×10^{-1}
Gliese 581	6	1.490×10^5	1.834×10^9	7.703×10^4	3.165×10^{-1}	2.216×10^{-1}
HD 191939	6	1.519×10^5	4.489×10^9	1.826×10^5	3.709×10^{-1}	4.311×10^{-1}
HD 34445	6	8.312×10^4	2.040×10^{10}	1.536×10^6	2.998×10^{-1}	1.809×10^{-1}
HD 40307	6	1.480×10^5	4.498×10^9	1.887×10^5	2.354×10^{-1}	1.409×10^{-1}
HIP 41378	6	1.137×10^5	1.195×10^{10}	6.600×10^5	2.535×10^{-1}	1.973×10^{-1}
K2-138	6	1.966×10^5	3.205×10^9	1.023×10^5	1.777×10^{-1}	1.574×10^{-1}
Kepler-11	6	1.187×10^5	9.041×10^9	4.783×10^5	1.561×10^{-1}	1.147×10^{-1}
Kepler-20	6	1.697×10^5	4.374×10^9	1.615×10^5	2.004×10^{-1}	5.286×10^{-2}
Kepler-80	6	2.077×10^5	2.250×10^9	6.805×10^4	1.788×10^{-1}	1.455×10^{-1}
Gliese 667 C (GJ 667 C)	7	8.712×10^4	5.863×10^9	4.225×10^5	1.772×10^{-1}	1.260×10^{-1}
HD 219134	7	2.141×10^5	2.042×10^9	5.940×10^4	3.857×10^{-1}	3.788×10^{-1}
tau Ceti	7	1.077×10^5	8.897×10^9	5.161×10^5	1.983×10^{-1}	1.936×10^{-1}
TRAPPIST-1	7	9.297×10^4	1.380×10^9	9.325×10^4	1.386×10^{-1}	4.525×10^{-2}
KOI-351	8	1.404×10^5	7.673×10^9	3.435×10^5	1.924×10^{-1}	1.636×10^{-1}

Table A1. Cont.

System Name	Nump.	v_0 (m/s)	R_0 (m)	T_0 (s)	λ	σ
HD 10180	9	2.504×10^5	2.225×10^9	5.566×10^4	2.813×10^{-1}	2.719×10^{-1}
Sun	10	6.364×10^4	3.255×10^{10}	3.204×10^6	2.681×10^{-1}	1.344×10^{-1}

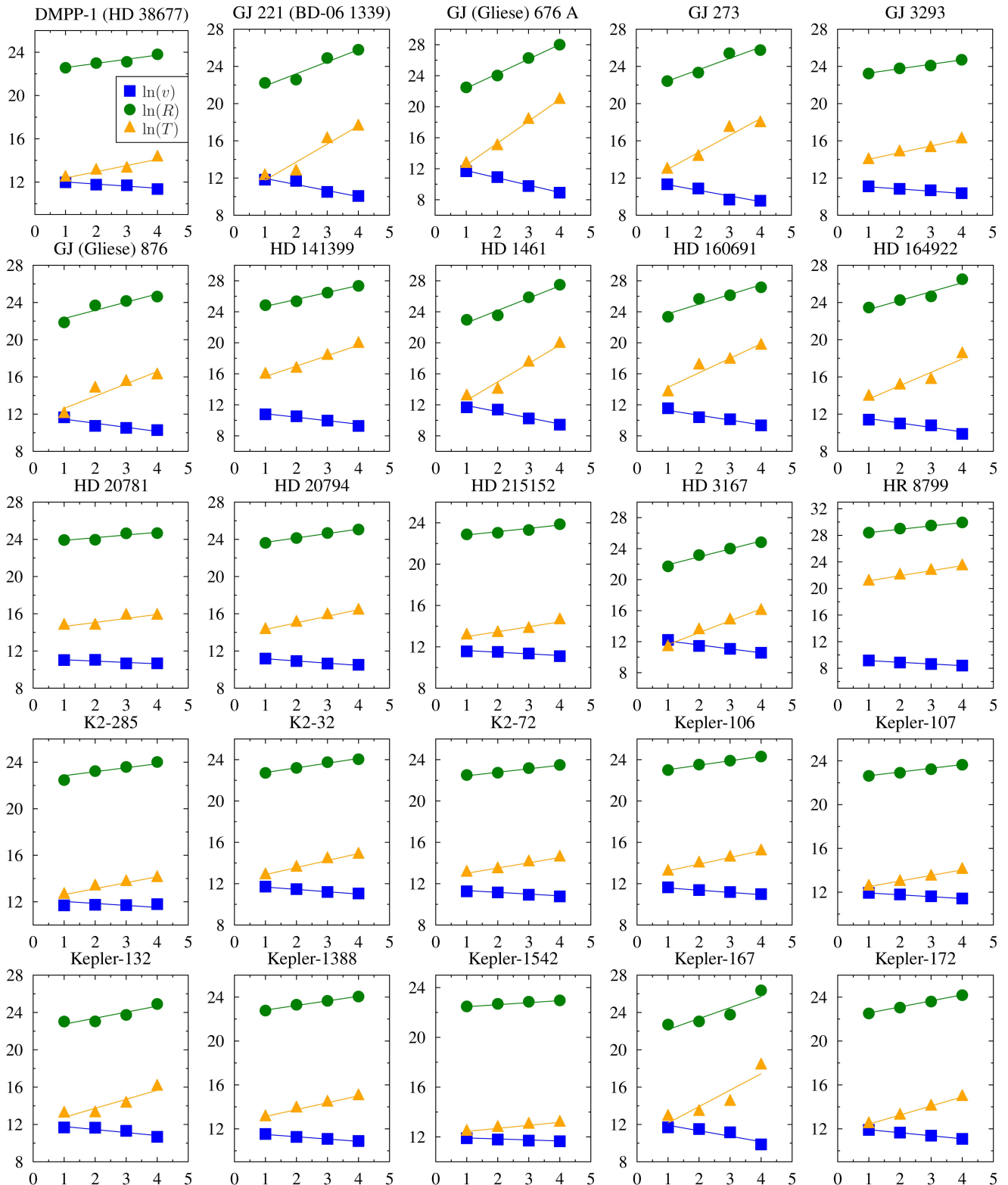


Figure A1. Logarithmic plots of three orbital parameters: velocity, semi-major axis, and period.

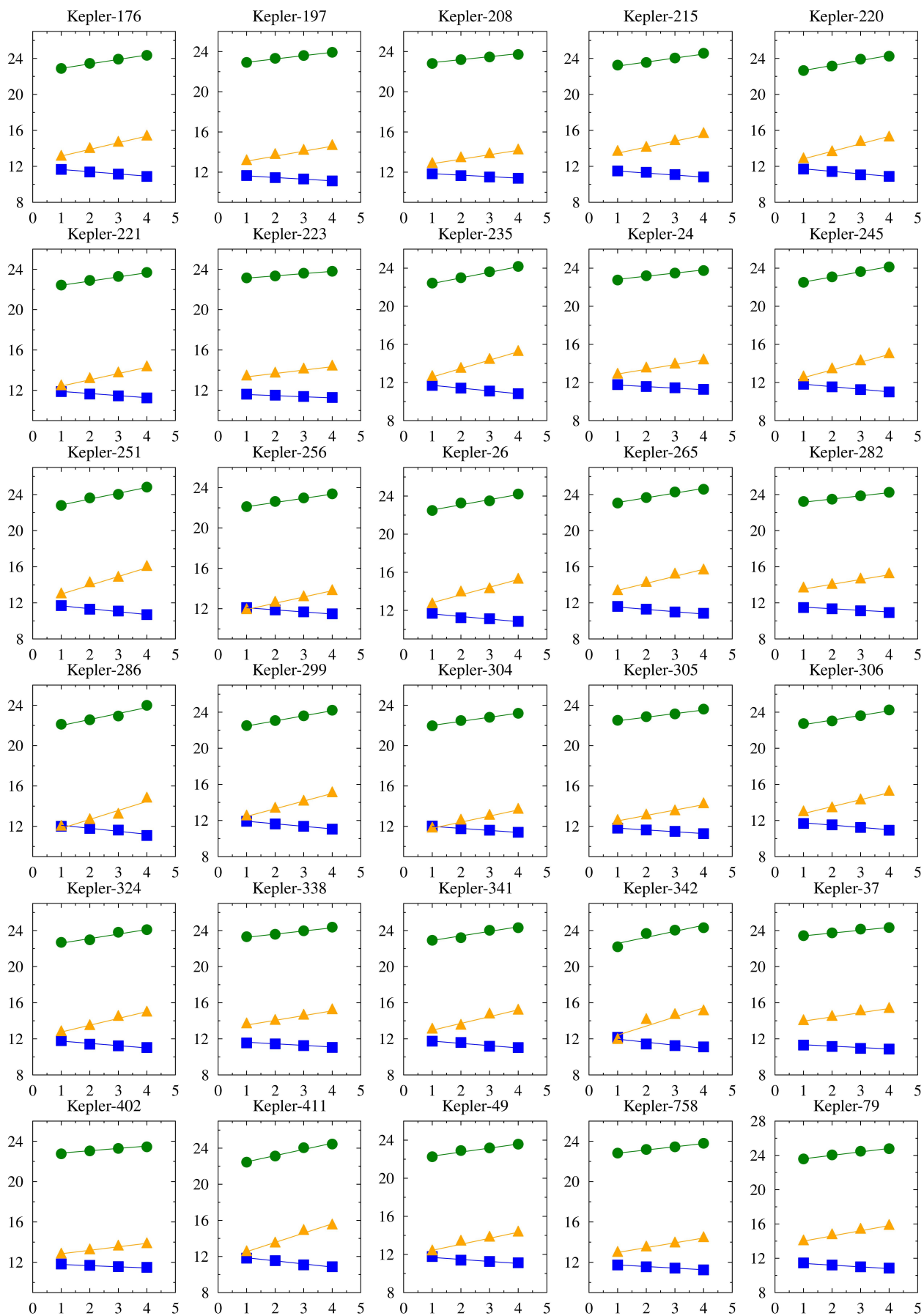


Figure A2. Logarithmic plots of three orbital parameters: velocity, semi-major axis, and period.

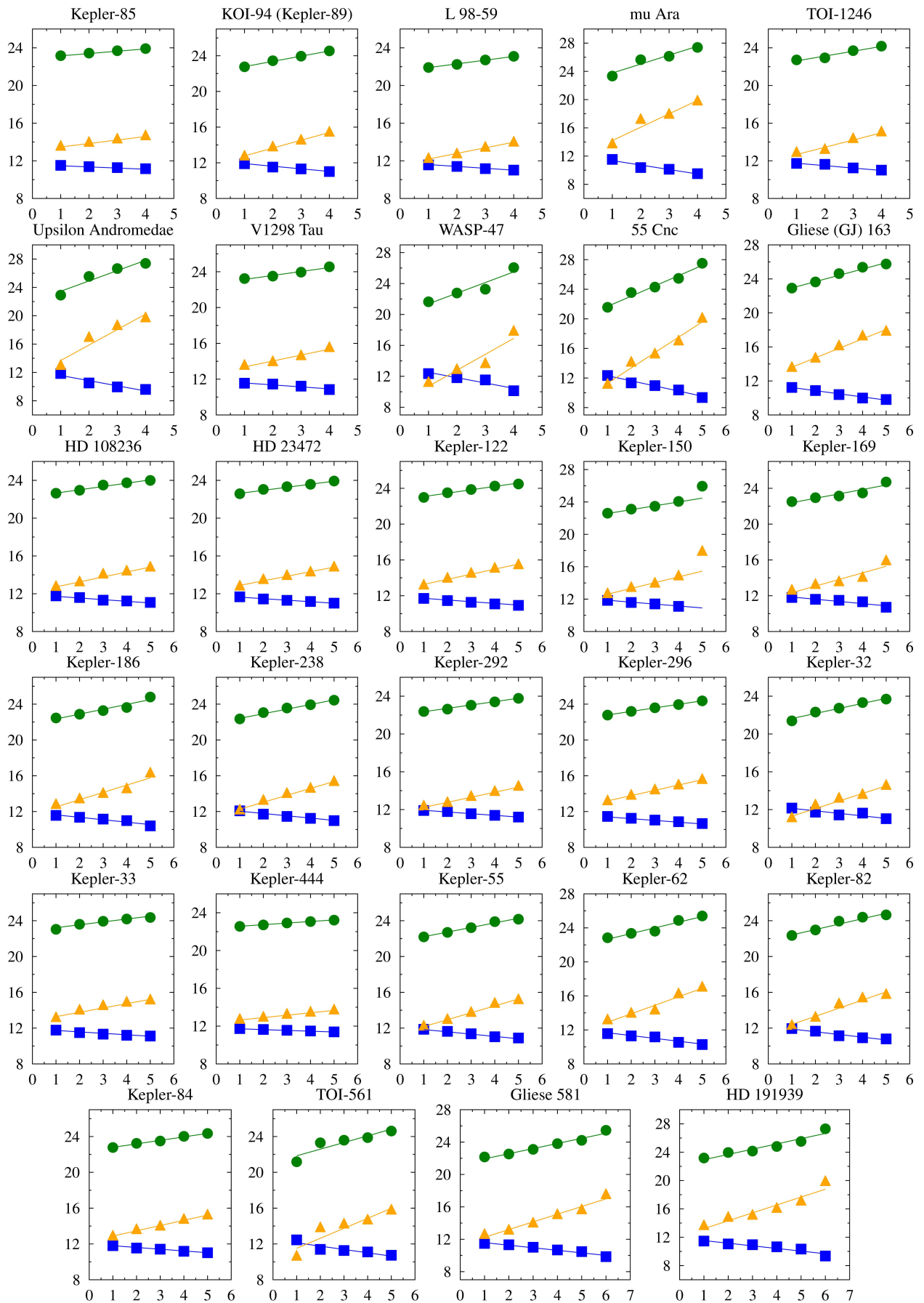


Figure A3. Logarithmic plots of three orbital parameters: velocity, semi-major axis, and period.

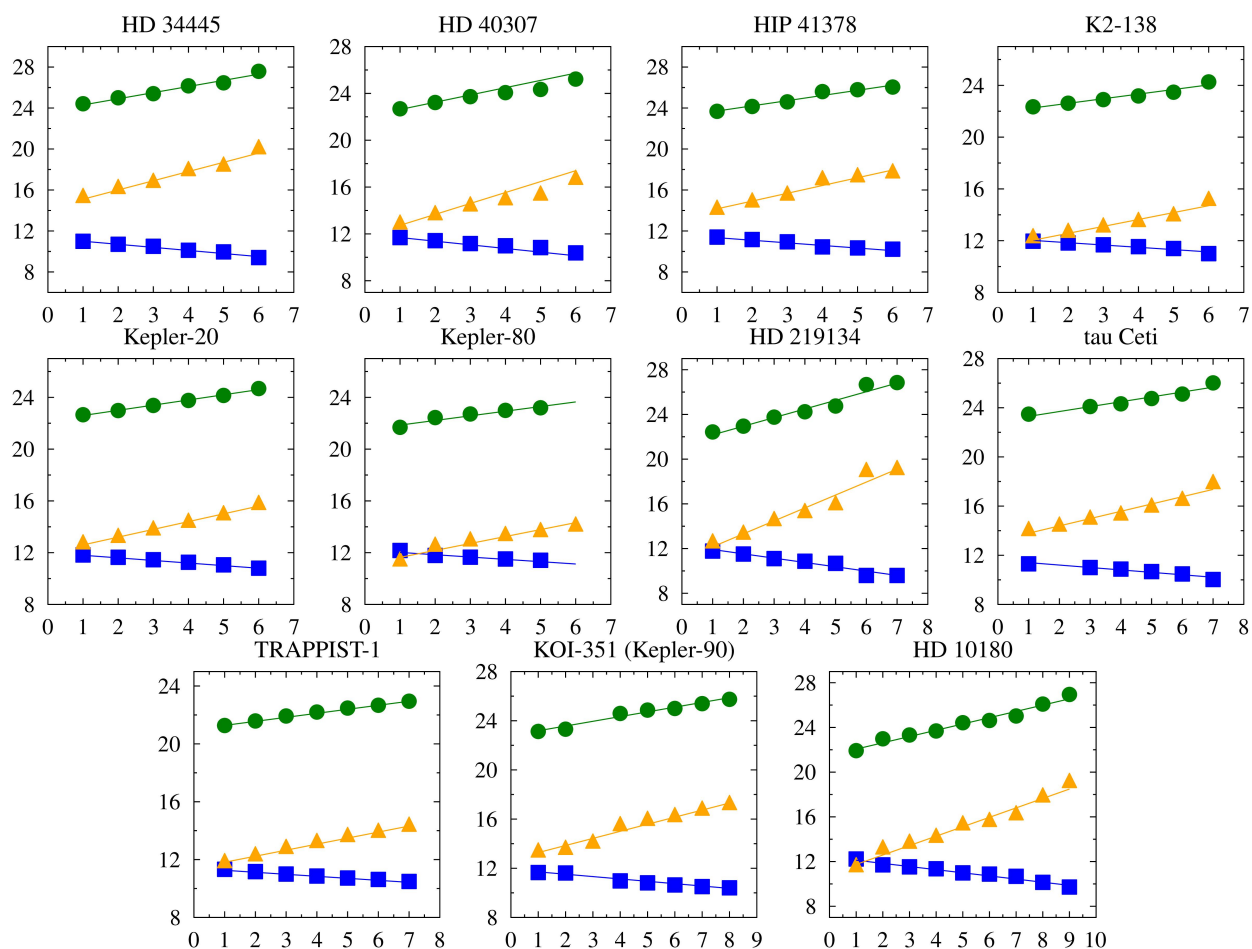


Figure A4. Logarithmic plots of three orbital parameters: velocity, semi-major axis, and period.

References

- Kepler, J. *Mysterium Cosmographicum*; ETH-Bibliothek Zürich: Tübingen, Germany, 1596.
- Kepler, J. *Astronomia Nova*; Translated by Casper, M.; Green Lion Press: Oldenburg, München, Germany, 1609.
- Kepler, J. *Harmonices Mundi*; Translated by Casper, M.; Linz: Oldenburg, München, Germany, 1619.
- Nieto, M. *The Titius-Bode Law of Planetary Distances: Its History and Theory*; Pergamon Press: Oxford, UK, 1972.
- Nieto, M. The letters between Titius and Bonnet and the Titius-Bode law of planetary distances. *Am. J. Phys.* **1985**, *53*, 22. [[CrossRef](#)]
- Barut, A.O. Symmetry and dynamics: Two distinct methodologies from Kepler to supersymmetry. In *Symmetries in Science II*; Plenum Press: New York, NY, USA, 1989; p. 37.
- Cseh, J. Planetary Systems and the Hidden Symmetries of the Kepler Problem. *Symmetry* **2020**, *12*, 2109. [[CrossRef](#)]
- Goldreich, P. An Explanation of the Frequent Occurrence of Commensurable Mean Motions in the Solar System. *Mon. Not. R. Astron. Soc.* **1965**, *130*, 159. [[CrossRef](#)]
- Dermott, S.F. On the Origin of Commensurabilities in the Solar System—II The Orbital Period Relation. *Mon. Not. R. Astron. Soc.* **1968**, *141*, 363. [[CrossRef](#)]
- Huang, C.; Bakos, G. Testing the Titius–Bode law predictions for Kepler multiplanet systems. *Mon. Not. R. Astron. Soc.* **2014**, *442*, 674–681. [[CrossRef](#)]
- Bovaird, T.; Lineweaver, C. Exoplanet predictions based on the generalized Titius–Bode relation. *Mon. Not. R. Astron. Soc.* **2013**, *435*, 1126. [[CrossRef](#)]
- Graner, F.; Dubrulle, B. Titius-Bode laws in solar system: I. Scale invariance explains everything. *Astron. Astrophys.* **1994**, *301*, 262.
- Graner, F.; Dubrulle, B. Titius-Bode laws in solar system: II. Build your own law from disk models. *Astron. Astrophys.* **1994**, *301*, 269.
- Buta, A. Toward an atomic model of the planetary system. *Rev. Romaine Phys.* **1982**, *27*, 321.
- Ragnarsson, S. Planetary distances: A new simplified model. *Astron. Astrophys.* **1995**, *282*, 609.
- Poveda, A.; Lara, P. The exo-planetary system of 55 Cancri and the Titius-Bode law. *Rev. Mex. Astron. Astrofis.* **2008**, *34*, 243.
- Lynch, P. On the significance of the Titius–Bode law for the distribution of the planets. *Mon. Not. R. Astron. Soc.* **2003**, *341*, 1174. [[CrossRef](#)]

18. Wybourne, B. *Classical Groups for Physicists*; Wiley: New York, NY, USA, 1974.
19. Fock, V. Zur Theorie des Wasserstoffatoms. *Z. Phys.* **1936**, *98*, 145. [[CrossRef](#)]
20. Bargmann, V. Zur Theorie des Wasserstoffatoms: Bemerkungen zur gleichnamigen Arbeit von V. Fock. *Z. Phys.* **1936**, *99*, 576. [[CrossRef](#)]
21. Györgyi, G. Kepler's Equation, Fock Variables, Bacry's Generators and Dirac Brackets. *Nuovo Cimento* **1968**, *53A*, 717. [[CrossRef](#)]
22. Györgyi, G. Kepler's Equation, Fock Variables, Bacry's Generators II. Classical and quantum group dynamics of the Kepler problem. *Nuovo Cimento* **1969**, *62A*, 449. [[CrossRef](#)]
23. Wulfman, C. *Dynamical Symmetry*; World Scientific: Singapore, 2011.
24. Barut, A.; Bohm, A.; Ne'eman, Y. *Dynamical Groups and Spectrum Generating Algebras*; World Scientific: Singapore, 1986.
25. Iachello, F.; Arima, A. *The Interacting Boson Model*; Cambridge University Press: Cambridge, MA, USA, 1987.
26. Quesne, C. Symmetry and Dynamical Lie Algebras in Classical and Quantum Mechanics. In *Symmetries in Physics*; Frank, A., Wolf, K., Eds.; Springer: Berlin/Heidelberg, Germany, 1992; p. 325.
27. Barut, A.; Bornzin, G. Unification of the external conformal symmetry group and the internal conformal dynamical group. *J. Math. Phys.* **1974**, *15*, 1000. [[CrossRef](#)]
28. NASA Exoplanet Archive, Which Is Operated by the California Institute of Technology, under Contract with the National Aeronautics and Space Administration under the Exoplanet Exploration Program. 2023. Available online: <https://exoplanetarchive.ipac.caltech.edu> (accessed on 9 January 2023).
29. Open Exoplanet Catalogue. 2023. Available online: <http://openexoplanetcatalogue.com> (accessed on 9 January 2023).
30. The Extrasolar Planets Encyclopaedia. 2023. Available online: <http://exoplanet.eu/catalog/> (accessed on 9 January 2023).
31. Exoplanet Orbit Database and Exoplanet Data Explorer. 2023. Available online: <http://exoplanets.org> (accessed on 9 January 2023).
32. Han, E.; Wang, S.X.; Wright, J.T.; Feng, Y.K.; Zhao, M.; Fakhouri, O.; Brown, J.I.; Hancock, C. Exoplanet Orbit Database. II. Updates to Exoplanets.org. *Publ. Astron. Soc. Pac.* **2014**, *126*, 827. [[CrossRef](#)]
33. Santerne, A.; Malavolta, L.; Kosiarek, M.R.; Dai, F.; Dressing, C.D.; Dumusque, X.; Hara, N.C.; Lopez, T.A.; Mortier, A.; Vanderburg, A.; et al. An extremely low-density and temperate giant exoplanet. *arXiv* **2019**, arXiv:1911.07355.
34. Stöcker, H.; Harris, J. *Handbook of Mathematics and Computational Science*; Springer: Berlin/Heidelberg, Germany, 1998; p. 386.
35. Xie, J.; Dong, S.; Zhu, Z.; Huber, D.; Zheng, Z.; De Cat, P.; Fu, J.; Liu, H.G.; Luo, A.; Wu, Y.; et al. Exoplanet orbital eccentricities derived from LAMOST-Kepler analysis. *Proc. Natl. Acad. Sci. USA* **2016**, *113*, 11431–11435. [[CrossRef](#)]
36. Goździewski, K.; Migaszewski, C. Multiple mean motion resonances in the HR 8799 planetary system. *Mon. Not. R. Astron. Soc.* **2014**, *440*, 3140–3171. [[CrossRef](#)]
37. Thompson, W.; Marois, C.; Do Ó, C.R.; Konopacky, Q.; Ruffio, J.B.; Wang, J.; Skemer, A.J.; De Rosa, R.J.; Macintosh, B. Deep Orbital Search for Additional Planets in the HR 8799 System. *Astron. J.* **2023**, *165*, 29. [[CrossRef](#)]

Disclaimer/Publisher's Note: The statements, opinions and data contained in all publications are solely those of the individual author(s) and contributor(s) and not of MDPI and/or the editor(s). MDPI and/or the editor(s) disclaim responsibility for any injury to people or property resulting from any ideas, methods, instructions or products referred to in the content.